0.1 MPM at ambient temperature shown in Figure 7, with T_1^{-1} being about four times faster for Cs–NH_3 solutions. This behavior indicates that, unlike the other alkalis, λ for Cs is sufficiently large for $T_{e\text{-}c}^{-1}$ to make the largest contribution to T_1^{-1} even in dilute solutions. This behavior has important implications for the nature of the solvated electron in dilute solutions, because it indicates that the electron is not completely dissociated from the cation. This result is consistent with the larger g shifts measured for Cs–NH_3 solutions at these concentrations. Using eq 5 and 7 and assuming that τ, δ, and Δ are cation independent makes it possible to estimate the change in relaxation rate expected from the corresponding g shifts for different cations. Since, at about 10^{-3} MPM, $\Delta g_{Cs} \simeq -2.3 \times 10^{-3}$ and $\Delta g_{Na} \simeq -1.1 \times 10^{-3}$, we estimate that $T_{e\text{-}Cs}^{-1}(SO)/T_{e\text{-}Na}^{-1}(SO) \simeq (\Delta g_{Cs}/\Delta g_K)^2 \simeq 4$, which is in reasonable agreement with experiment.

At higher concentrations the evidence for spin–orbit relaxation in Cs–NH_3 solutions is even more compelling. As shown in Figures 7 and 8, T_1^{-1} begins to increase at a concentration that is about one order of magnitude lower than that of the lighter alkalis and increases even more dramatically at higher concentrations ($\gtrsim$1 MPM). Again, these enhancements in relaxation rate undoubtedly result from efficient spin–orbit relaxation due to the large λ of Cs. The initial increase in T_1^{-1} above about 0.1 MPM probably corresponds to the formation of associated species, whereas the more pronounced increase above about 1 MPM most likely reflects the onset of electron delocalization.[14] In support of the latter hypothesis, extrapolation of the relaxation time at 248 K in Figure 7 to 14 MPM yields $T_1 \simeq 10^{-11}$ s, which is in good agreement with the value of T_1 for a 14 MPM Cs–NH_3 solution obtained independently by extrapolating the relaxation data for metallic 14 MPM Na–, K–, and Rb–NH_3 solutions,[17] where we have shown that the dominant spin–lattice relaxation mechanism is provided by the motional modulation of the spin–orbit coupling between the conduction electrons (e_m) and solvated cations. In a metal the spin–orbit relaxation rate is given by[17]

$$T_{e_m\text{-}c}^{-1}(SO) = (\Delta g)^2/\tau_R = Ne^2(\Delta g)^2/\alpha\sigma m^* \quad (9)$$

where τ_R is the resistivity relaxation time ($\tau_R \simeq 10^{-3}$ s for a 5 MPM Cs–NH_3 solution at 240 K), m^* is the effective mass of the conduction electrons ($m^* = m$ for a free electron), and α is a constant. The g shift is given by $\Delta g = \lambda/\Delta E$, where E is the energy difference to the nearest band with the same transformation properties as the one of interest. When eq 5, 7, and 9 are compared, it is evident that the expressions for spin–orbit relaxation are formally quite similar for nonmetallic and metallic solutions. If we neglect any variations in N and m^* at different concentrations in the more concentrated Cs–NH_3 solutions, it follows from eq 9 that $\sigma T_1^{-1}/(\Delta g)^2$ should be a constant if the spin–orbit mechanism predominantes. Unfortunately, it is not possible to determine the ratio unambiguously because the electrical conductivity below 7 MPM has not been measured.

Finally, we discuss briefly the temperature dependence of the relaxation rate. As shown in Figure 9, in the dilute range ($\lesssim$0.1 MPM), T_1^{-1} decreases with increasing temperature, which indicates that $T_{e\text{-}N}^{-1}(SO)$ makes an important contribution to T_1^{-1} (see eq 8). However, the change in T_1^{-1} is only about half that for the lighter alkalis, which is again consistent with a substantial contribution of $T_{e\text{-}Cs}^{-1}(SO)$ to the relaxation rate in the dilute range. In agreement with our conclusions based on the concentration dependence of T_1^{-1}, at higher Cs concentrations the rapid increase in T_1^{-1} with increasing temperature clearly illustrates that spin–orbit relaxation is dominant (see eq 8).

Acknowledgment. This research was supported by grants from the Science and Engineering Research Council, NATO, and by National Science Foundation Grant No. DMR 79-21069, DMR 75-09215, and DMR 82-15315.

Registry No. Ce, 7440-46-2; NH_4^+, 7664-41-7.

Fluorescence Studies on the Characterization and Solubilizing Abilities of Sodium Dodecyl Sulfate, Hexadecyltrimethylammonium Chloride, and Triton X-100 Micelles

Koji Kano,* Yoshiyuki Ueno, and Shizunobu Hashimoto

Department of Applied Chemistry, Faculty of Engineering, Doshisha University, Kamikyo-ku, Kyoto 602, Japan *(Received: December 7, 1984)*

The relationship between solubilizing ability and characteristics of a micelle has been studied. Triton X-100 micelles solubilized hydrophobic solute such as tetratolylporphine (TTP) and *N*-methyl-*N*-hexylaniline (MHA) much more efficiently than sodium dodecyl sulfate (SDS) and hexadecyltrimethylammonium chloride (HTAC) micelles. In order to understand the extremely high solubilizating ability of Triton X-100 micelle, the microscopic fluidity and polarity of the micellar interior were compared with those of SDS and HTAC micelles. The fluorescence of dipyrenylpropane, which shows an intramolecular excimer emission, indicated that the micellar interior of Triton X-100 was much more viscous than those of SDS and HTAC. The emission from dansyldodecylamine suggested that the more rigid micellar structure of Triton X-100 provides a less polar environment. These observations can be well interpreted in terms of an oblate ellipsoid model for the Triton X-100 micelle. It seems that the hydrophobic core of the Triton X-100 micelle prefers to incorporate TTP. Analyses of the fluorescence decay curves of pyrene in micelles containing MHA as a quencher suggested that the aggregation number of the Triton X-100 micelle decreases continuously with increasing amount of incorporated MHA while no morphological change occurs in the SDS micellar system. The structurally flexible nature of the Triton X-100 micelle may realize the incorporation of large amounts of MHA.

Introduction

In a previous paper, we reported that Triton X-100 micelles solubilize very hydrophobic compounds such as 1,3-bis(1-pyrenyl)propane (P(3)P) and 5,10,15,20-tetrakis(*p*-tolyl)porphine (TTP) while ionic surfactant micelles formed by sodium dodecyl sulfate (SDS) and hexadecyltrimethylammonium chloride (HTAC) do not.[1] The solubility in micelles should be affected by the physical properties of both micelle and solute which dominate the stability of the solute-embedded micelle. It is very important to apply an accurate micelle model when discussing the solubilizing ability of micelles. There are four models for ionic

(1) Kano, K.; Ueno, Y.; Umakoshi, K.; Hashimoto, S.; Ishibashi, T.; Ogawa, T. *J. Phys. Chem.* **1984**, *88*, 5087.

0022-3654/85/2089-3161$01.50/0

surfactant micelles: (1) the classical Hartley model,[2] (2) the porous cluster model,[3] (3) the surfactant-block model,[4] and (4) the statistical lattice model.[5] On the basis of the results on the hydration numbers of micellar aggregates, the Menger's porous cluster model has been criticized.[6] Most of the results on the microscopic polarities of micelles obtained from absorption and fluorescence spectroscopy, however, suggest that lots of water molecules penetrate into the spherical ionic micelles leading to relatively polar micellar interiors.[7-13] Of course, the probe method contains serious problems. One of them is the binding site of the probe molecules in the micelle. Perturbation of the micropscopic environment of a micelle by the probe molecule may also provide inaccurate information on the microscopic polarity of the micelle itself. It should be recognized that the probe molecules yield information on the physical property or properties of the microscopic environment of micelle where the probe molecules are located. The probe method, however, seems to be very useful for studying the solubilizing abilities of micelles because probe molecules can be regarded as solute molecules. If the microscopic environment of the micelle where very hydrophobic solute molecule is located is very polar, such solute-embedded micelles should be thermodynamically unstable leading to poor solubility of the solute in the micelles. It is reasonable to assume that the microscopic fluidity of the micelle affects the microscopic polarity of the micelle because the more fluctuant nature of the micelle leads to a more polar environment of the micelle. In the present study, we measured the microscopic polarities and fluidities of the ionic and nonionic micelles, which may dominate the solubilizing abilities, by using the fluorescent probe method.

The relative size of the solute molecules and the micelle may be another factor affecting the solubility. From a CPK molecular model, a van der Waals radius and a long axis dimension of the TTP molecule are estimated as 8[14] and ca. 22 Å, respectively. It is likely that the TTP molecule is too large to be embedded in spherical micelles having an average radii of 12–30 Å.[15] If these assumptions are correct, Triton X-100 micelles should have a large micelle size and a more hydrophobic environment. Recently, Robson and Dennis[16] and Paradies[17] have postulated an oblate ellipsoid model for the Triton X-100 micelle. Employing an average molecular weight (MW) of 90 000 (aggregation number (AN) = 140), Robson and Dennis[16] have calculated half-axis dimensions for the oblate ellipsoid micelle to be 27 Å × 52 Å which are in good agreement with the results of a small-angle X-ray scattering analysis done by Paradies.[17] This model predicts a more hydrophobic and more viscous core for the Triton X-100 micelle because of its well-packed structure. The MW of the Triton X-100 micelle has been determined by light scattering,[18] and ultracentrifugation techniques.[19] All of these studies indicate that Triton X-100 forms considerably large micelles (MW = 63000–150000) compared with ionic micelles (MW = 18000 for SDS and 26000 for HTAC). The nature of the Triton X-100 micelle may be interpreted from the higher ability of this molecule to solubilize hydrophobic and/or large solute molecules.

The aim of the present study is to clarify the factors which dominate the ability of a micelle to solubilize very hydrophobic and/or large solute molecules.

TABLE I: Critical Micelle Concentrations (cmc) of Surfactants and Aggregation Numbers (AN) of Micelles at Room Temperature

surfactant	cmc, M	AN
SDS	8.2×10^{-3} [a]	62[a]
HTAC	1.0×10^{-3} [b]	80[b]
Triton X-100	3.2×10^{-4} [c]	140[d]

[a] Mysels, K. J.; Princen, L. H. *J. Phys. Chem.* **1959**, *63*, 1696. [b] Atik, S. S.; Singer, A. *Chem. Phys. Lett.* **1978**, *59*, 519. [c] Reference 1. [d] Reference 18b.

Experimental Section

Materials. P(3)P was available from the previous work.[1] TTP was prepared and purified according to the procedures described in the literature.[20] *N*-Methyl-*N*-hexylaniline (MHA) was prepared by refluxing a mixture of *N*-methylaniline, hexyl bromide, and potassium carbonate in ethanol for 10 h. The crude MHA was purified by silica gel column chromatography with cyclohexane–chloroform (1:1). Dansyldodecylamine (DDA) was prepared by stirring an equimolar mixture of dodecylamine and dansyl chloride in methanol containing potassium carbonate for 1 h. The crude DDA was chromatographed on silica gel by using benzene as an eluent. Surfactants were the same as those used in the previous work.[1]

Solubilization of TTP and MHA in Micelles. An appropriate volume of the stock solution of TTP in chloroform or MHA in methanol was placed in a test tube and the solvent was removed by a stream of nitrogen gas. The residue was added to 5 mL of aqueous micellar solution and sonicated (a Bransonic 12, 50 W) for 30 (TTP) or 5 min (MHA) at room temperature. The relative degree of solubilization of TTP was determined by measuring the fluorescence spectrum of TTP by exciting at 413 nm and that of MHA was evaluated from the turbidity of the micellar solution which was measured by transmittance at 500 nm. The turbidity measurement indicated that the solubility limit of MHA in water is 3×10^{-5} M. The solution became turbid at MHA concentrations above 3×10^{-5} M. Fluorescence and absorption spectra were taken on a Hitachi 650-60 spectrofluorimeter (excitation and emission bandwidths = 2 nm) and a Shimadzu UV200S spectrophotometer, respectively, whose cell compartments were thermostated at 25 °C.

Fluorescence Spectra of P(3)P. The stock solution of P(3)P in acetone was injected into an appropriate volume of aqueous micellar solution to adjust [P(3)P] = 1×10^{-6} M. The micellar solution was deaerated by freeze–pump–thaw nitrogen gas charge treatment (six cycles). Beside deaeration, the freeze–thaw treatment is very important to establish the solute–micelle equilibrium as mentioned previously.[1] The fluorescence spectra of P(3)P were taken on a Shimadzu RF-500 spectrofluorimeter at 25 °C by exciting P(3)P at 345 nm. Excitation and emission bandwidths were 3 and 5 nm, respectively. The method for measuring the fluorescence decay curves was the same as that described previously.[1]

Fluorescence Quenching. An appropriate volume of the stock solution of MHA in methanol was added to the micellar solution of pyrene (5×10^{-6} M) and sonicated at room temperature for 5 min. The sample was deaerated by evacuating the system and admitting nitrogen gas (ten cycles). Pyrene was excited at 339 nm and the fluorescence intensities of the pyrene monomer were followed at 372 nm with a Hitachi 650-60 spectrofluorimeter.

(2) Hartley, G. S. *Q. Rev. Chem. Soc.* **1948**, *2*, 152.
(3) Menger, F. M. *Acc. Chem. Res.* **1979**, *12*, 111. Menger, F. M.; Chow, J. F. *J. Am. Chem. Soc.* **1983**, *105*, 5501.
(4) Fromherz, P. *Chem. Phys. Lett.* **1980**, *77*, 460.
(5) Dill, K. A.; Flory, P. J. *Proc. Natl. Acad. Sci. U.S.A.* **1981**, *78*, 676.
(6) Wennerström, H.; Lindman, B. *J. Phys. Chem.* **1979**, *83*, 2931.
(7) Fendler, J. H.; Fendler, E. J.; Infante, G. A.; Shih, P. S.; Patterson, L. K. *J. Am. Chem. Soc.* **1975**, *97*, 89.
(8) Kalyanasundaram, K.; Thomas, J. K. *J. Phys. Chem.* **1977**, *81*, 2176.
(9) Mukerjee, P.; Cardinal, J. R. *J. Phys. Chem.* **1978**, *82*, 1620.
(10) Zachariasse, K. A.; Phuc, N. V.; Kozankiewicz, B. *J. Phys. Chem.* **1981**, *85*, 2676.
(11) Kano, K.; Goto, H.; Ogawa, T. *Chem. Lett.* **1981**, 653.
(12) Ramachandran, C.; Pyter, R. A.; Mukerjee, P. *J. Phys. Chem.* **1982**, *86*, 3198.
(13) Russell, J. C.; Whitten, D. G. *J. Am. Chem. Soc.* **1982**, *104*, 5937.
(14) Yamada, S.; Sato, T.; Kano, K.; Ogawa, T. *Photochem. Photobiol.* **1983**, *37*, 257.
(15) Fendler, J. H.; Fendler, E. J. "Catalysis in Micellar and Macromolecular Systems"; Academic Press: New York, 1975; Chapter 2.
(16) Robson, R. J.; Dennis, E. A. *J. Phys. Chem.* **1977**, *81*, 1075. Robson, R. J.; Dennis, E. A. *Acc. Chem. Res.* **1983**, *16*, 251.
(17) Paradies, H. H. *J. Phys. Chem.* **1980**, *84*, 599.
(18) (a) Monkowich, A. M. *J. Phys. Chem.* **1954**, *58*, 1027. (b) Kushner, L. M.; Hubbard, W. D. *Ibid.* **1954**, *58*, 1163. (c) Kuriyama, K. *Kolloid Z.* **1962**, *181*, 144.
(19) Dwiggins, C. W.; Bolen, R. J.; Dunning, H. N. *J. Phys. Chem.* **1960**, *64*, 1175.
(20) Little, R. G.; Anton, J. A.; Loach, P. A.; Ibene, J. A. *J. Heterocyl. Chem.* **1975**, *12*, 343. Adler, A. D.; Longo, F. R.; Kampas, F.; Kim, J. *J. Inorg. Nucl. Chem.* **1970**, *32*, 2443.

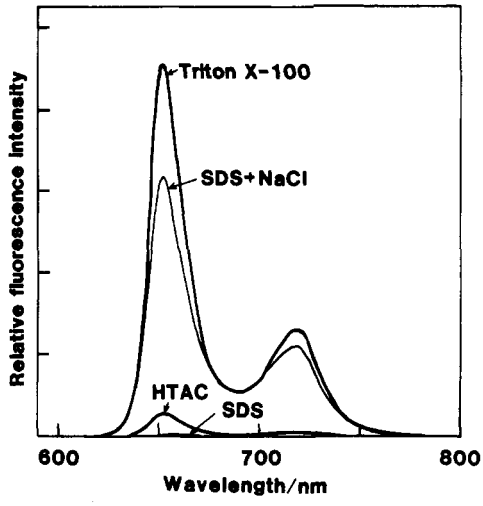

Figure 1. Fluorescence spectra of TTP (5×10^{-6} M) in Triton X-100, HTAC, and SDS micellar solutions. The micelle concentrations were 5×10^{-5} M except for the SDS–NaCl system. The effect of NaCl was measured for the 6.9×10^{-2} M SDS solution containing 0.6 M NaCl. TTP was excited at 413 nm.

Fluorescence decay curves of the pyrene monomer were taken on an Ortec-PRA single-photon-counting apparatus. All measurements were undertaken at 25 °C.

Results

Solubilization of TTP and MHA in Micelles. In order to determine the ability of nonionic and ionic micelles to solubilize hydrophobic solutes, we incorporated TTP and MHA into Triton X-100, SDS, and HTAC micelles according to the procedures described in the Experimental Section.

TTP is a large planar molecule, the van der Waals radius being ca. 8 Å.[14] TTP is so hydrophobic that it exists as a nonfluorescent solid dispersed in water. As TTP is solubilized in micelles, fluorescence having maximum intensities at 654 and 720 nm appears. Figure 1 shows the fluorescence spectra of TTP (5×10^{-6} M) in Triton X-100, SDS, and HTAC micellar solutions. Since the solubility depends on the micelle concentration, the micelle concentration of each sample was adjusted to 5×10^{-5} M by using the parameters listed in Table I. As shown in Figure 1, the fluorescence intensities of TTP in Triton X-100 solution was much larger than those in SDS and HTAC solutions, suggesting that Triton X-100 micelles solubilize TTP much more efficiently than SDS and HTAC micelles. The absorption spectrum of TTP in the Triton X-100 micellar solution was virtually the same as those in homogeneous organic solvents while TTP in SDS and HTAC solutions showed very weak and broad absorption bands (Figure 2). This indicates that TTP in 5×10^{-5} M SDS and HTAC micellar solutions exists predominantly in an aggregate form. The fluorescence intensities of TTP did not change 1 day after the SDS and HTAC solutions of TTP were prepared. These results show the very poor abilities of SDS and HTAC micelles to solubilize TTP. Even if the micelle concentration increased to 9.8×10^{-4} M ([SDS] = 6.9×10^{-2} M), TTP was scarecely incorporated in SDS micelles. Addition of 0.6 M NaCl to the SDS (6.9×10^{-2} M) solution, however, caused a marked enhancement of the solubilization as shown in Figure 1. It has been reported that the spherical micelle of SDS (6.9×10^{-2} M) changes its morphology to a rodlike micelle upon addition of NaCl (0.6 M).[21] The morphological change accompanying the change in physical properties of the SDS micelle should provide the NaCl-induced enhancement of the solubilization of TTP.

MHA is a surfactant-like molecule without charge. Figure 3 shows the differences in the abilities to solubilize MHA between above three surfactant micelles ([micelle] = 1.5×10^{-5} M). The term $\bar{n}_0$ denotes the average number of MHA molecules in a micelle which is calculated by assuming that the aggregation number (AN) of the micelle does not change upon addition of MHA. The micelle parameters listed in Table I were used for calculating $\bar{n}_0$. The solubilities were followed by measuring the turbidities of the micellar solutions. The solubility limit of MHA in water was 3×10^{-5} M. In the presence of micelles, the solubility limits increased to 0.014 ([MHA]/[surfactant] = 0.14), 0.034 (0.28), and 0.23 M (1.1) for the SDS, HTAC, and Triton X-100 solutions, respectively. At MHA concentrations above the solubility limits, the surfactant solutions were emulsified and the turbidities of the solutions drastically increased. The solubilizing abilities decreased in the order of Triton X-100, HTAC, and SDS, which is consistent with the order of the decrease of the solubilities of TTP. The data show the extremely large ability of Triton X-100 micelles to solubilize MHA. Similar to the case of TTP, the solubility of MHA in SDS (6.9×10^{-2} M) micelles also increased upon addition of 0.6 M NaCl (Figure 3). Although it has been reported that the AN of the SDS micelle changes from 62 to ca. 1000 upon addition of NaCl under the present conditions,[21] $\bar{n}_0$ in Figure 3 was calculated by using an AN of 62 for comparison.

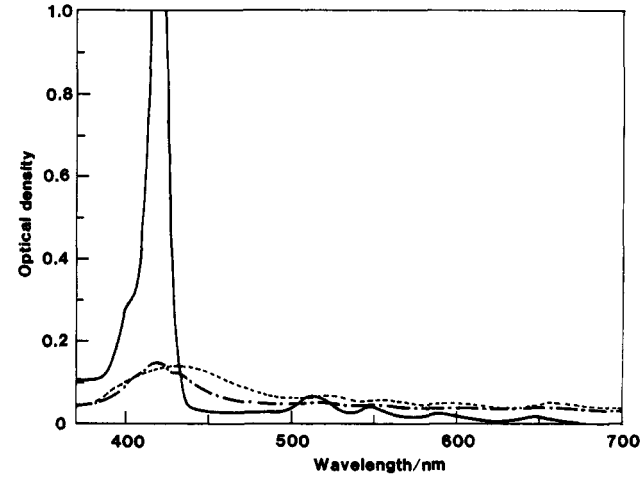

Figure 2. Absorption spectra of TTP (5×10^{-6} M) in Triton X-100 (—), HTAC (-·-), and SDS (---) micellar solutions ([micelle] = 5×10^{-5} M).

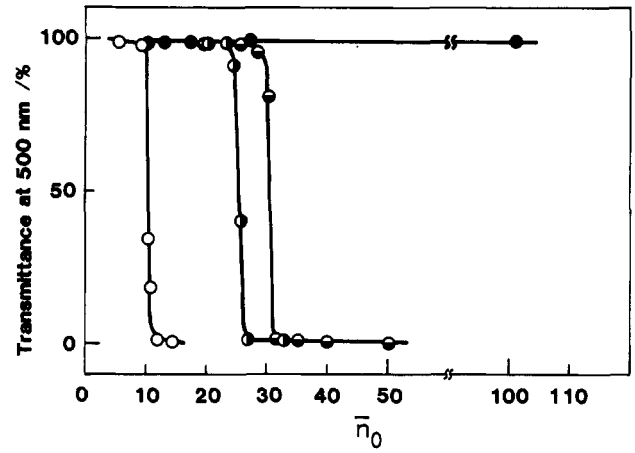

Figure 3. Turbidity changes of 0.21 M Triton X-100 (●), 0.12 M HTAC (◑), and 0.1 M SDS (○) solutions at 500 nm upon addition of MHA. The micelle concentrations were 1.5×10^{-3} M in all cases. The effect of NaCl was measured for the 6.9×10^{-2} M SDS solution containing 0.6 M NaCl (◒). $\bar{n}_0$ is the mean number of MHA molecules per micelle calculated by assuming that each micelle does not change its morphology upon addition of MHA. The micelle parameters for calculation of $\bar{n}_0$ are listed in Table I.

Fluorescence of P(3)P. Fluidities of Micellar Interiors. It is well-known that pyrene in the singlet excited state collides with that in the ground state leading to the formation of an excimer state which shows a broad and structureless band at longer wavelength. Since the formation of the pyrene excimer is a diffusion-controlled process, an attempt has been carried out to

(21) Mazer, N. A.; Benedek, G. B.; Carey, M. C. *J. Phys. Chem.* **1976**, *80*, 1075.

TABLE II: I_M/I_E and t_L Values of P(3)P in Various Micellar Solutions at 25 °C

surfactant	concn	I_M/I_E	t_L, ns
Triton X-100[a]	4.5×10^{-3} M	4.5	98
Triton X-405[b]	3.5×10^{-2} M	3.8	89
Emulgen 911[c]	1 mg/mL	3.3	81
Tween 80[d]	3.0×10^{-3} M	1.7	74
Brij 58[e]	8.0×10^{-4} M	1.8	70
Brij 35[f]	1.3×10^{-3} M	1.8	60
HTAC	1.0×10^{-2} M	1.3	45
SDS	1.0×10^{-2} M	0.81	43

[a] Polyoxyethylene(9.5) *p-tert*-octylphenyl ether. [b] Polyoxyethylene-(40) *p-tert*-octylphenyl ether. [c] Polyoxyethylene nonylphenyl ether. [d] Polyoxyethylene(20) sorbitan monooleate. [e] Polyoxyethylene(20) hexadecyl ether. [f] Polyoxyethylene(23) dodecyl ether.

study the fluidities of micellar interiors by analyzing the pyrene fluorescence.[22] It should be noted, however, that a statistical distribution of pyrene molecules among micelles has to be considered for intermolecular excimer formation. Intramolecular excimer systems, where two fluorescent groups are linked with an alkyl chain, have been employed as improved fluorescent probes for evaluation of the microscopic viscosities of micelles and liposomes.[23] We used P(3)P as a viscosity-sensitive fluorescent probe. The alkyl chain of P(3)P in the ground state preferentially takes an all-trans conformation which should change to the eclipsed form to yield an intramolecular excimer state (E*) via a locally excited state (M*). It is expected, therefore, that the fluorescence intensity of the intramolecular excimer of P(3)P decreases and t_L increases with increasing viscosity of the medium, where t_L is the time difference between the maxima of the excimer fluorescence intensity and the exciting light pulse. The t_L value can be determined from the rise and decay curves of the intramolecular excimer emission of P(3)P.

Much attention should be payed to the solubilization of P(3)P in micelles because of the very slow solubilization. It has been known that P(3)P exists initially as microcrystals in the HTAC and SDS solutions without any treatment.[1] The P(3)P–micelle equilibrium state was realized by applying a freeze–thaw effect on the solubilization observed previously by us.[1] Table II shows the ratios of the intensities of the fluorescence from M* to those from E* (I_M/I_E) and t_L in various nonionic, HTAC, and SDS micelles. A very clear rise and decay curve for the intramolecular excimer fluorescence of P(3)P was observed for each system, indicating that most of the P(3)P molecules are included in the micelles under these conditions. Both I_M/I_E and t_L values in the nonionic micelles were larger than those in HTAC and SDS micelles, suggesting that intramolecular excimer formation of P(3)P in nonionic micelles is restricted compared with that in ionic micelles. These results suggest that the micellar interiors of the nonionic surfactants where the P(3)P molecules are located are less fluid than those of HTAC and SDS. Especially, the Triton X-100 micelle seems to have a very viscous interior. Lianos et al. also measured the fluorescence of P(3)P in ionic micellar solutions to study a specific interaction between quaternary ammonium groups of cationic micelles and arenes.[24] These authors reported the I_M/I_E value for the HTAC micelle to be 3.7 which is much larger than ours (1.3). We could not reproduce their result under various conditions.

Fluorescence of DDA. Polarities of Micellar Interiors. Aminonaphthalene derivatives have been widely used as fluorescent probes to show the microscopic polarities of micelles, liposomes, polymers, enzymes, and so on. 1-Anilinonaphthalene-8-sulfonate (ANS) is a typical fluorescer whose fluorescence maximum shifts to longer wavelength and the fluorescence quantum yield decreases with increasing polarity of the medium. Since ANS is a water-soluble compound, however, it can be used for limited conditions. Then we prepared DDA as a probe which is incorporated into micelles and does not interact electrostatically with the heat groups of ionic micelles.

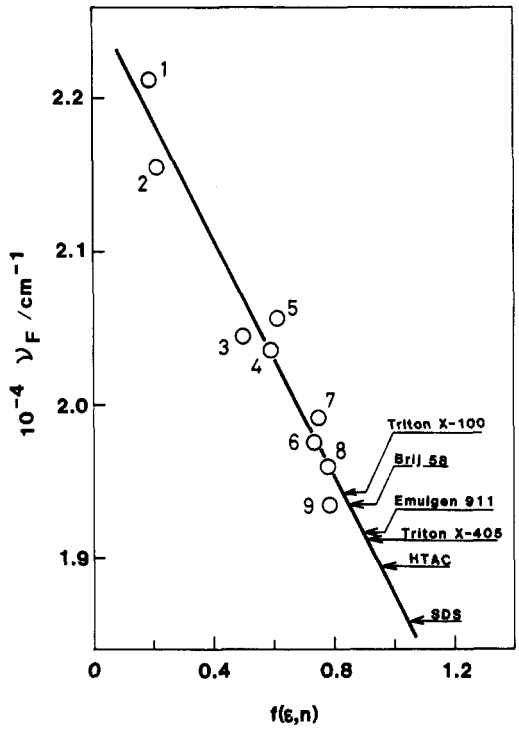

Figure 4. Plot of ν_F of DDA vs. $f(\epsilon,n)$ for organic solvents and the estimated polarities of various micellar interiors: 1, hexane; 2, cyclohexane; 3, chloroform; 4, ethyl acetate; 5, tetrahydrofuran; 6, 2-propanol; 7, acetone; 8, ethanol; and 9, methanol.

Figure 4 shows a relationship between the energy of the fluorescence maximum of DDA (ν_F) and the solvent polarity parameter ($f(\epsilon,n)$):[25]

$$f(\epsilon,n) = 2(\epsilon - 1)/(2\epsilon + 1) - (n^2 - 1)/(2n^2 + 1) \quad (1)$$

where ϵ and n are the dielectric constant and the refractive index of the solvent, respectively. A fairly good linear relationship between ν_F and $f(\epsilon,n)$ can be used as a calibration curve for estimating the relative polarity of the site in the micelle where the dimethylaminonaphthalene moiety is located. The ν_F values of DDA in the micellar solutions are shown in Figure 4, which indicates that nonionic micelles provide less polar environments compared with ionic micelles.

Since DDA consists of a hydrophobic alkyl chain and a rather hydrophilic dimethylaminonaphthalene moiety, it is expected that the fluorescent moiety is located near the surface of the micelle. The DDA fluorescence, therefore, may be affected by the polarities around micellar surfaces. The results shown in Figure 4 suggest that the surfaces of all micelles are more polar than ethanol. The polarities of the micellar surfaces increased in the order Triton X-100, HTAC, and SDS, which is the same order as the increase in the fluidities of the micellar interiors. Estimation of the microscopic polarities of micelles has been examined by measuring the fluorescence spectra of 1-pyrenecarboxaldehyde[8] and *N,N*-dimethyl-4-[3-(1-pyrenyl)]aniline[11] and the absorption spectra of benzophenone,[7] 2,2,6,6-tetramethylpiperidinyl-1-oxy,[12] and 2,6-diphenyl-4-(2,4,6-triphenyl-1-pyridino)phenoxide.[10] All of these results are consistent with those obtained in this study.

Fluorescence Quenching of Pyrene by MHA. Morphological Change of Triton X-100 Micelle. It has been well established that solute molecules are distributed among micelles according to Poisson statistics.[26] In the case of fluorescence quenching of

(22) Pownall, H. J.; Smith, L. C. *J. Am. Chem. Soc.* **1973**, *95*, 3136.
(23) (a) Zachariasse, K. A. *Chem. Phys. Lett.* **1978**, *57*, 429. (b) Emert, J.; Behrens, C.; Goldenberg, M. *J. Am. Chem. Soc.* **1979**, *101*, 771. (c) Turro, N. J.; Aikawa, M.; Yekta, A. *Ibid.* **1979**, *101*, 772. (d) Zachariasse, K. A.; Kühnle, W.; Weller, A. *Chem. Phys. Lett.* **1980**, *73*, 6.
(24) Lianos, P.; Viriot, M.-L.; Zana, R. *J. Phys. Chem.* **1984**, *88*, 1098.
(25) Lippert, E. *Z. Naturforsch. A* **1955**, *10*, 541. Lippert, E. *Electrochem.* **1957**, *61*, 962. Mataga, N.; Kaifu, Y.; Koizumi, M. Bull. *Chem. Soc. Jpn.* **1955**, *28*, 690. Mataga, N.; Kaifu, Y.; Koizumi, M. *Ibid.* **1956**, *29*, 465.

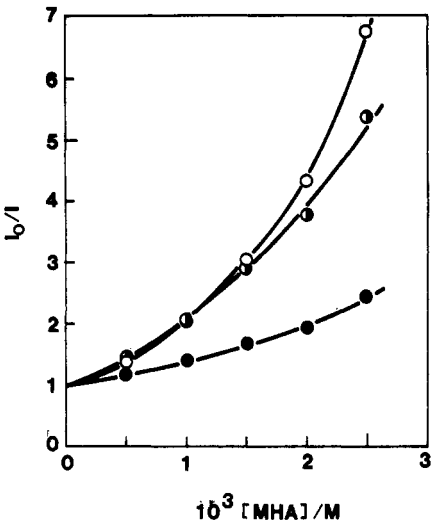

Figure 5. Plots of I_0/I vs. [MHA] for Triton X-100 (●), HTAC (◑), and SDS (○) solutions. The micelle concentrations were 1.5×10^{-3} M in all cases.

pyrene by MHA, the statistical distribution of the quencher molecules (MHA) among micelles provides the following equation for the time-resolved fluorescence intensity of pyrene ($I(t)$):[27]

$$I(t) = I(0) \exp[\bar{n}(e^{-k_1 t} - 1) - k_0 t] \quad (2)$$

where $I(0)$ is the fluorescence intensity at $t = 0$, k_0 is the first-order rate constant for fluorescence decay of pyrene in the absence of quencher, and k_1 is the first-order rate constant for intramicellar fluorescence quenching in micelles containing one quencher molecule. The term $\bar{n}$ represents the average number of quencher molecules per micelle:

$$\bar{n} = [\text{quencher}]/[\text{micelle}] \quad (3)$$

Equation 2 can be used only for the case where the quencher molecules are located preferentially in micelles. A water-insoluble quencher, MHA, is adequate to apply this kinetics. The fluorescence intensity measured by steady-state fluorimetry can be expressed by

$$I/I_0 = \sum_{n=0}^{\infty} \frac{\bar{n}(e^{-\bar{n}}/n!)}{1 + n(k_1/k_0)} \quad (4)$$

where I_0 and I are the fluorescence intensities of pyrene in the absence and in the presence of MHA, respectively.

In this study, the initial micelle concentrations of SDS, HTAC, and Triton X-100 were adjusted to 1.5×10^{-3} M. Figure 5 shows plots of I_0/I vs. [MHA] in micellar solutions. As is expected from eq 4, the plots of I_0/I vs. [MHA] did not obey a simple Stern–Volmer linear relationship. The quenching efficiency in the Triton X-100 micellar solution was much lower than those in the SDS and HTAC micellar solutions. As Figure 6 shows, the fluorescence decay curves in the presence of MHA were not single exponential in all cases (the data for the HTAC solutions are not shown herein). The experimentally obtained decay curves for the SDS and Triton X-100 solutions were fitted to the theoretical curves calculated by using eq 2 and k_1 and n as parameters. The theoretical curves shown by the solid lines in Figure 6 were well fitted with the experimental results. The k_1 and n values thus obtained are summarized in Table III together with the micelle concentrations calculated from eq 3 and AN calculated from

$$\text{AN} = \frac{[\text{surfactant}] - \text{cmc}}{[\text{micelle}]} \quad (5)$$

(26) Tachiya, M. *Chem. Phys. Lett.* **1975**, *33*, 289. Rodgers, M. A. J.; Da Silva e Wheeler, M. F. *Ibid.* **1978**, *53*, 165. Yekta, A.; Aikawa, M.; Turro, N. J. *Ibid.* **1979**, *63*, 543. Infelta, P. P. *Ibid.* **1979**, *61*, 88.
(27) Waka, Y.; Hamamoto, K.; Mataga, N. *Chem. Phys. Lett.* **1979**, *62*, 364.

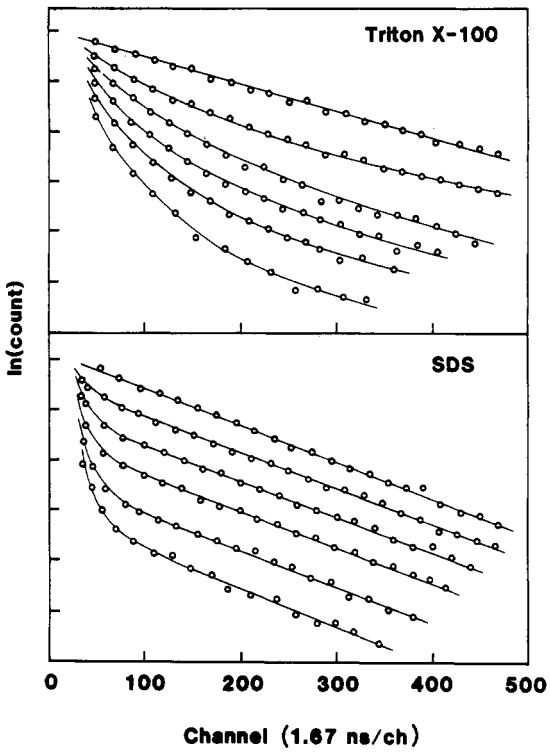

Figure 6. Fluorescence decay curves for the pyrene monomer in Triton X-100 and SDS micellar solutions ([micelle] = 1.5×10^{-3} M) with and without MHA. 10^3[MHA] = 0, 0.5, 1.0, 1.5, 2.0, and 2.5 M (from the top). The solid lines are the theoretical decay curves calculated by using eq 2 and k_1 and $\bar{n}$ values listed in Table III.

TABLE III: Rate Constants for Fluorescence Decays of Pyrene in the Absence of Quencher (k_0), First-Order Rate Constants for Intramicellar Fluorescence Quenching of Pyrene by MHA (k_1), Average Numbers of MHA per Micelle ($\bar{n}$), Micelle Concentrations ([micelle]), and Aggregation Numbers of Micelles (AN) Obtained from Analyses of the Fluorescence Decay Curves of Pyrene in SDS and Triton X-100 Micelles Containing MHA

10^3[MHA], M	$10^{-6}k_0$, s^{-1}	10^7k_1, s^{-1}	$\bar{n}$	10^3[micelle], M	AN
		SDS			
0	4.3		0	1.5	62[a]
0.5		2.6	0.37	1.4	67
1.0		2.7	0.85	1.2	77
1.5		2.7	1.2	1.2	77
2.0		2.6	1.7	1.2	77
2.5		2.6	2.1	1.2	77
		Triton X-100			
0	3.1		0	1.5	140[b]
0.5		0.4	0.30	1.7	122
1.0		0.4	0.55	1.8	114
1.5		0.5	0.65	2.3	91
2.0		0.5	0.75	2.7	77
2.5		0.5	0.87	2.9	71
5.0		0.5	1.5	3.3	63

[a] Mysels, K. J.; Princen, L. H. *J. Phys. Chem.* **1959**, *63*, 1696. [b] References 18b.

where cmc is the critical micelle concentration. We could not fit the fluorescence decay curves for the HTAC solutions.

One of the interesting aspects derived from Table III is that the AN of the Triton X-100 micelle decreases with increasing quencher concentration while that of the SDS micelle is essentially constant. Another notable result is that the intramolecular fluorescence quenching rate constant, k_1, for Triton X-100 micelles are much smaller than those for SDS micelles. The k_1 value may be affected by two factors, micelle size and microscopic viscosity of the micellar interior. Judging from the fact that the k_1 values for the Triton X-100 micelle does not change significantly even if the AN is reduced (see Table III), it seems that the k_1 value

is affected predominantly by the microscopic viscosity of the micelle. The smaller k_1 values for Triton X-100 micelles may be ascribed to the more rigid interiors of these micelles compared with SDS micelles. This aspect is consistent with that obtained from P(3)P fluorescence measurements (vide supra).

Discussion

One of the important functions of surfactant micelles is the solubilization of hydrophobic compounds in their interiors. The solubility in a micelle depends on many factors, i.e., shape of micelle and solute molecules, hydrophobicity of the micellar interior, polarity and polarizability of the solute, charge-transfer interaction between the micelle and solute, hydrogen-bonding ability, the counterion of micelle, surfactant concentration, and so on. Ultimately, it can be concluded that the solubility of a certain compound in a micelle depends on the free energy of the solute in the micelle.[28] The present paper deals with the solubilization of very hydrophobic compounds (TTP and MHA), which are almost insoluble in water, in micelles and the factors affecting the solubilities of these compounds in micelles. As a first approximation, the micelle core can be regarded as an oil droplet. For such a case, a hydrophobic solute molecule can be found at any place in the micelle core. An absolute small-angle X-ray scattering have shown the diameters of the cores of SDS and HTAC micelles as 35.6 and 43.4 Å, respectively.[29] Since the long-axis dimension of TTP is estimated as 22 Å from the CPK molecular model, it is expected that a TTP molecule can be incorporated in these micelle cores if the cores can be regarded as hydrocarbon-like oil droplets. The present results show, however, that TTP is scarcely incorporated in these micelles. The fluorescence of P(3)P and DDA suggested that the micellar interiors of SDS and HTAC where the probe molecules are located are considerably fluid and polar compared with that of Triton X-100. A spherical micelle retains its structure because of the balance of the attractive force from the hydrophobic effect and repulsive force from the hydrophilic head groups.[30] If a large and structurally rigid solute molecule such as TTP is located at the center of the micelle core, the hydrophobic interaction between the alkyl chains of surfactant molecules may be perturbed greatly. TTP, therefore, may be incorporated in a palisade layer. Judging from the relative size of TTP and the ionic micelles, a considerable part of the TTP molecule will be exposed to a very polar environment in the vicinity of the micelle–water interface. Consequently, it is assumed that TTP in SDS and/or HTAC micelles has a large free energy and exists preferentially as a solid in these micellar solutions.

It has been well established by light scattering and ultracentrifugation techniques that Triton X-100 forms considerably large micelles (MW = 63000–150000).[18,19] A spherical structure is not adequate for the Triton X-100 micelle because it requires mixing of the hydrophobic octyl phenyl groups and the hydrophilic polyoxyethylene groups. Recently, Robson and Dennis[16] and Paradies[17] have postulated an oblate ellipsoid model for the Triton X-100 micelle. According to this model, the hydrophobic groups and the hydrophilic groups of Triton X-100 can separate from each other and each layer packs well. As the fluorescence of P(3)P and DDA shows, the interior of the Triton X-100 micelle is less fluid and less polar than those of the SDS and HTAC micelles, which can be interpreted reasonably by the oblate ellipsoid model. The half-axis dimensions of the whole Triton X-100 micelle and of the hydrophobic core formed by the octyl phenyl groups have been estimated as 27 Å × 52 Å and 14.5 Å × 39.5 Å, respectively.[16] Such a large ellipsoidal core allows solubilization of a large molecule such as TTP. Since the average curvature of the external surface area of the Triton X-100 micelle is so small (28 Å),[17] water penetration into the micelle should be prevented. The hydrophobic core of the Triton X-100 micelle prefers to solubilize hydrophobic TTP. The NaCl-enhanced solubilization of TTP in SDS micelles confirms the assumption that the solubility of TTP in the micelle greatly depends on the polarity of the micellar interior. Neutralization of the anionic charge of the SDS micelle by Na^+ causes the formation of a large aggregate (rodlike micelle) because the repulsive force due to the charged head groups is reduced.[21] It it quite reasonable to consider that the micellar interior of the rodlike micelle is less polar than that of the spherical micelle.

Another notable nature of the Triton X-100 micelle is its morphological change upon solubilization. The AN values of Triton X-100 and SDS micelles under the conditions given were determined by the fluorescent quenching method.[31] The reliability of this method was confirmed by the fact that the AN's of the Triton X-100 and SDS micelles without solute, which were estimated by extrapolation, were almost the same as the reported values. As Table III shows, the AN of the Triton X-100 micelle decreased continuously with increasing incorporated MHA (quencher) while no morphological change was observed for the SDS micellar system under these conditions. The solubilities of MHA in micelles were much different between Triton X-100 and SDS (see Figure 1). A SDS micelle can embed only 9 molecules of MHA, whereas a Triton X-100 micelle is stable untill it incorporates 150 molecules of MHA. The SDS micelle seems to be structurally inflexible, which may cause the fragile nature toward external perturbations. On the contrary, it seems that the Triton X-100 micelle is structurally flexible and changes its morphology to reconstruct a thermodynamically stable conditions when solute molecules are added into the system. As the SDS micelle includes the MHA molecules, the surface area available per charged head group will increase.[32] The micellar structure retained by a balance between attractive and repulsive forces will destruct when large amounts of the MHA molecules are included. Meanwhile, the repulsive force of nonionic micelles is much small than those of ionic micelles. This may cause the structurally flexible nature of the Triton X-100 micelle. In the present study, the morphological change of the Triton X-100 micelle could be followed only for the case where the MHA concentrations are relatively low (see Table III). The morphology of Triton X-100 micelle including large amounts of MHA molecules cannot be deduced from the present results. It may be possible to form mixed micelles or microemulsions consisting of Triton X-100 and large amounts of MHA.

Acknowledgment. This work was partially supported by the Asahi Glass Foundation for Industrial Technology.

Registry No. SDS, 151-21-3; CTAC, 112-02-7; TTP, 14527-51-6; MHA, 30189-89-0; Triton X-100/X-405, 9002-93-1; Emulgen 911, 9016-45-9; Tween 80, 9005-65-6; Brij 58, 9004-95-9; Brij 35, 9002-92-0; dipyrenylpropane, 79480-81-2; dansyldodecylamine, 96446-07-0.

(28) Almgren, M.; Grieser, F.; Thomas, J. K. *J. Am. Chem. Soc.* **1979**, *101*, 279.
(29) Reiss-Husson, F.; Luzzati, V. *J. Phys. Chem.* **1964**, *68*, 3504.
(30) Tanford, C. J. *J. Phys. Chem.* **1974**, *78*, 2469.
(31) Atik, S. S.; Thomas, J. K. *J. Am. Chem. Soc.* **1981**, *103*, 7403. Kano, K.; Yamaguchi, T.; Ogawa, T. *J. Phys. Chem.* **1984**, *88*, 793.
(32) Almgren, M.; Swarup, S. *J. Colloid Interface Sci.* **1983**, *91*, 256.